Proceedings of the ASME 2019 38th International Conference on Ocean, Offshore and Arctic Engineering
OMAE2019
June 9-14, 2019, Glasgow, Scotland

OMAE2019-95249

HYBRID METHOD FOR PREDICTING SHIP MANOEUVRABILITY IN REGULAR WAVES

Tianlong Mei[1]
School of Naval Architecture, Ocean and Civil Engineering, Shanghai Jiao Tong University
Shanghai, China
Maritime Technology Division, Ghent University
Belgium

Yi Liu
School of Naval Architecture, Ocean and Civil Engineering, Shanghai Jiao Tong University
Shanghai, China
Marine Design and Research Institute of China
Shanghai, China

Manasés Tello Ruiz, Marc Vantorre, Evert Lataire, Changyuan Chen
Maritime Technology Division, Ghent University
Belgium

Zaojian Zou
State Key Laboratory of Ocean Engineering, Shanghai Jiao Tong University,
Shanghai, China
School of Naval Architecture, Ocean and Civil Engineering, Shanghai Jiao Tong University
Shanghai, China

ABSTRACT

The ship's manoeuvring behaviour in waves is significantly different from that in calm water. In this context, the present work uses a hybrid method combining potential flow theory and Computational Fluid Dynamics (CFD) techniques for the prediction of ship manoeuvrability in regular waves. The mean wave-induced drift forces are calculated by adopting a time domain 3D higher-order Rankine panel method, which includes the effect of the lateral speed and forward speed. The hull-related hydrodynamic derivatives are determined based on a RANS solver using the double body flow model. The two-time scale method is applied to integrate the improved seakeeping model in a 3-DOF modular type Manoeuvring Modelling Group (MMG model) to investigate the ship's manoeuvrability in regular waves.

Numerical simulations are carried out to predict the turning circle in regular waves for the S175 container carrier. The turning circle's main characteristics as well as the wave-induced motions are evaluated. A good agreement is obtained by comparing the numerical results with experimental data obtained from existing literature by Yasukawa [1][2]. This demonstrates that combining potential flow theory with CFD techniques can be used efficiently for predicting the manoeuvring behaviour in waves. This is even more true when the manoeuvring derivatives cannot be obtained from model tests when there is lack of such experimental data.

1 INTRODUCTION

The need for a more realistic prediction of the ship manoeuvrability when navigating and manoeuvring in coastal or harbour areas has stressed the importance to incorporate wave effects in mathematical manoeuvring models. Moreover, the effect of waves on a manoeuvring ship is also an important focus reflected by Energy Efficient Design Index (EEDI), which has been put into force by the International Maritime Organization (IMO) for CO2 emissions allowance and the maximum installed power on-board.

Despite the high cost of experimental studies, free-running model tests in waves are considered to be the most accurate method to estimate wave effects on ship manoeuvring. Such tests have been carried out by many researchers, such as Ueno et al. [3], Lee et al. [4], Yasukawa et al. [5]. Recently, Sprenger et al.[6] conducted a benchmark experimental study on ship manoeuvring in waves in the frame of the SHOPERA project. Although the last decades witnessed the rapid development of high performance computers, the direct RANS-based CFD simulation still requires a significant amount of computing resources and is time-consuming too. This makes extremely hard to directly simulate ship manoeuvring in waves using CFD. To the author's best knowledge, only few researchers had performed direct CFD simulations. E.g. Mousaviraad et al. [7] conducted simulations for turning circle and zigzag manoeuvres of a transformable craft

[1] Contact author: Tianlong.Mei@UGent.be

(T-Craft) vessel based on URANS solver CFDship-Iowa. Cura et al. [8] studied the manoeuvrability of the DTC container ship in waves by using OpenFOAM. Wang et al. [9][10] carried out zigzag manoeuvres of a free running ship in waves using naoe-FOAM-SJTU.

In literature one can find mathematical models which are widely used to predict the ship manoeuvring in waves, e.g. Bailey et al. [11], Fossen [12], Sutulo and Soares [13], Schoop-Zipfel and Abdel-Maksoud [14], Subramanian and Beck [15]. In the studies mentioned above, the "unified method", which considers the memory effect or nonlinear factors due to the transient body wetted surface, is used to integrate manoeuvring and seakeeping problems. But the lack in their researches is that the second order wave forces is not accurately considered. Other researchers explored a different approach, the "two-time scale method" which subdivide the manoeuvring in waves problem in a seakeeping and a manoeuvring in calm water modules. In this method the second order wave forces are calculated by the seakeeping module beforehand and transfer to the manoeuvring model, while the kinematic parameters are computed by the manoeuvring module and transferred to the seakeeping module. This process is repeated at two different time scales. Examples of this method can be found in Skejic and Faltinsen [16] where they proposed the two-time scale method in regular waves, and Yasukawa et al. [17] where they studied the ship manoeuvring in regular and irregular waves and calculated the second order force by using different methods.

In [16] and [17] the major drawback in their studies is that the seakeeping problem was calculated using two dimensional approaches (2D strip theory). In Seo and Kim [18], Seo et al. [19], however, they applied the Neumann-Kelvin linearization based on the 3D Rankine panel method for a turning test of the S175 container ship in regular waves. Zhang et al. [20] modified the method in [18] by considering the lifting effects for the turning and zigzag manoeuvres prediction of the S-175 container ship in regular waves.

In spite of the differences between the unified and the two-time scale methods, the viscous hydrodynamic derivatives are almost always obtained from existing experiments. Recently, Chillcce and el Moctar [21] developed a numerical method to simulate the ship manoeuvring in waves. The viscous hydrodynamic coefficients are obtained by using CFD method and the second order wave drift forces are approximately expressed as a continuous function with respect to surge velocity and wave angle, which is computed beforehand by using the Rankine panel method and saved as database. The major problem with this approach is that the lateral speed and yaw angular velocity have not been considered in the estimation of the second order forces. However, according to the research in [19], the simulation results considering the lateral speed show better agreement with the experimental data.

In the present research, the turning circle main characteristics as well as the wave-induced motions of a S175 container ship are evaluated. The mean wave-induced drift forces, including the effect of the lateral speed and forward speed, are evaluated by adopting a time domain 3D higher-order Rankine panel method using double body basis flow, while the hull-related viscous hydrodynamic derivatives are determined based on a RANS solver using the double body flow model. The validation of the present method is carried out by comparing the numerical results with experimental data obtained from [1], [2].

2. MATHEMATICAL FORMULATION

Consider a ship moving with a velocity U, drift angle β and heading angle ψ_0 in the regular waves with wave angle χ, as depicted in Figure 1. $O-XYZ$ and $o-xyz$ mean global and body-fixed coordinate system, respectively. The x-axis coincides with the forward speed u and the origin o is located at the centre of gravity. The y-axis points portside, the Z and z axes points upward. The relationship of the two coordinate systems can be derived as follows:

$$\begin{aligned} X &= xcos\psi_0(t) - ysin\psi_0(t) + X_0(t) \\ Y &= xsin\psi_0(t) + ycos\psi_0(t) + Y_0(t) \\ Z &= z \end{aligned} \tag{1}$$

where $X_0(t)$ and $Y_0(t)$ denote the ship position without the oscillation component in the global coordinate system at time t. In this study, the manoeuvring problem is solved in the $O-XYZ$, whereas the wave induced motion is analysed in the body-fixed coordinate system $o-xyz$.

The incident wave potential in $o-xyz$ can be expressed as:

$$\varphi_I = \frac{\zeta_A g}{\omega_W} e^{kZ}[kxcos(\chi-\psi_0(t)) + kysin(\chi-\psi_0(t)) + kX_0(t)cos\chi + kY_0(t)sin\chi - \omega_W t] \tag{2}$$

where ζ_A is the wave amplitude, ω_W is the incident wave frequency, k is the wave number. From the Eq. (2), the encounter frequency ω_E can be derived as:

$$\omega_E = \omega_W - k[ucos(\chi-\psi_0(t)) + vsin(\chi-\psi_0(t))] \tag{3}$$

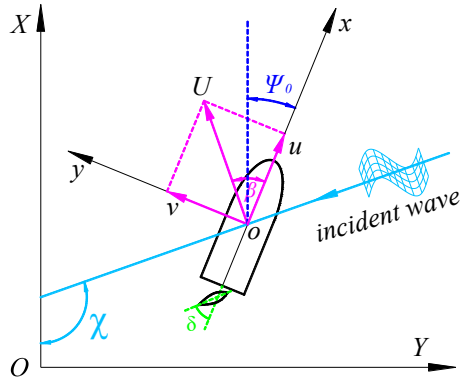

FIGURE 1: COORDINATE SYSTEMS

2.1 High Frequency Seakeeping Problem

In the frame of potential theory, the total velocity potential and wave elevation can be written as:

$$\Psi(\vec{x},\mathrm{t}) = \phi_s(\vec{x}) + \varphi_I(\vec{x},\mathrm{t}) + \varphi_d(\vec{x},\mathrm{t}) \quad (4)$$

$$\zeta(\vec{x},\mathrm{t}) = \zeta_I(\vec{x},\mathrm{t}) + \zeta_d(\vec{x},\mathrm{t}) \quad (5)$$

where ϕ_s is the basic velocity potential, φ_I is the regular incoming wave potential and ζ_I is the wave elevation. φ_d and are the disturbance velocity potential and ζ_d is the disturbance wave elevation.

In present study, the double body linearization is used, then the linearized Boundary Value Problem (BVP) of $\varphi_d(\vec{x},\mathrm{t})$ can be expressed as follows:

$$\nabla^2\varphi_d = 0, \text{ in the fluid domain;} \quad (6)$$

The kinematic and dynamic free surface conditions on free surface $\mathrm{z} = 0$ are:

$$\left[\frac{\partial}{\partial \mathrm{t}} - \left(\vec{U} - \nabla\phi_s\right)\cdot\nabla\right]\zeta_d = \frac{\partial\varphi_d}{\partial z} + \frac{\partial^2\varphi_d}{\partial z^2}\zeta - \nabla\phi_s\cdot\nabla\zeta_I \quad (7)$$

$$\left[\frac{\partial}{\partial \mathrm{t}} - \left(\vec{U} - \nabla\phi_s\right)\cdot\nabla\right]\varphi_d = -g\zeta_d - \nabla\phi_s\cdot\nabla\zeta_I + \vec{U}\cdot\nabla\phi_s - \frac{1}{2}\nabla\phi_s\cdot\nabla\phi_s \quad (8)$$

The body surface condition on the mean body surface $\vec{S}_b$ is:

$$\frac{\partial\varphi_d}{\partial n} = \sum_{j=1}^{6}(\dot{\xi}_j n_j + \xi_j m_j) - \frac{\partial\varphi_I}{\partial n}, \quad (9)$$

where $(m_1, m_2, m_3) = (\vec{n}\cdot\nabla)(\vec{U} - \nabla\phi_s)$, $(m_4, m_5, m_6) = (\vec{n}\cdot\nabla)[\vec{x}\times(\vec{U} - \nabla\phi_s)]$. Translation vector $\vec{\xi}_T = (\xi_1, \xi_2, \xi_3)$, rotation vector $\vec{\xi}_R = (\xi_4, \xi_5, \xi_6)$. The detailed evaluation of the m_j terms can be found in Mei et al [22].

In fact, when a ship sails in a real sea state or manoeuvres in waves, the lateral drift will be induced by the wave drifting forces, the occurrence of the lateral forces then produce considerable influence on the ship's motions, which will be different from the straight course case. To this end, the time domain 3D higher-order Rankine panel program in present study will consider the effects of forward speed and lateral speed for the laterally drifting ship in regular waves. Therefore, the velocity $\vec{U}$ in m_j, in Eq. (9), contains not only the effect of forward speed u, but also including the lateral speed v and yaw rate r, expressed as follows:

$$\vec{U} = (u - ry)\vec{\imath} + (v + rx)\vec{\jmath} + 0\vec{k} \quad (10)$$

Once the unknown velocity potentials are obtained, the hydrodynamic force and moment $F_i(\dot{\xi}_j, \xi_j, t)$ can be evaluated by:

$$F_i = -\iint_{\vec{S}_b}\rho\left[\frac{\partial}{\partial \mathrm{t}} - \left(\vec{U} - \nabla\phi_s\right)\cdot\nabla\right]\varphi_{I,d}\, n_i ds, i = 1\sim6, \quad (11)$$

The 6-DOF ship motion equations can be obtained base on Newton's second law,

$$M_{ij}\ddot{\xi}_j(t) + C_{ij}\xi_j(t) = F_i\left(\dot{\xi}_j, \xi_j, t\right), \qquad i,j = 1\sim6, \quad (12)$$

where M_{ij} and C_{ij} represent mass and restoring coefficients matrix, respectively.

In present study, the second-order wave force is evaluated by applying the pressure integration method, expressed as:

$$\begin{aligned}
\vec{F}^{(2)} &= -\rho\iint_{\vec{S}_b}\nabla\left(\frac{\partial}{\partial t} - \left(\vec{U} - \nabla\phi_s\right)\cdot\nabla\varphi\right)\cdot\vec{\delta}\ \vec{n}_0 ds \\
&-\rho\iint_{\vec{S}_b}\vec{H}\vec{x}\cdot\nabla\left(\vec{U}\cdot\nabla\phi_s + \frac{1}{2}\nabla\phi_s\cdot\nabla\phi_s + gz\right)\vec{n}_0 ds \\
&-\rho\iint_{\vec{S}_b}\frac{1}{2}\nabla\varphi\cdot\nabla\varphi\,\vec{n}_0 ds \\
&-\rho\iint_{\vec{S}_b}\left[\frac{\partial\varphi}{\partial t} - \vec{U}\cdot\nabla\varphi + \nabla\phi_s\cdot\nabla\varphi + g(\xi_3 + \xi_4 y - \xi_5 x)\right]\cdot\vec{n}_1 ds \\
&-\rho\iint_{\vec{S}_b}\left[\nabla\left(-\vec{U}\cdot\nabla\varphi + \frac{1}{2}\nabla\phi_s\cdot\nabla\phi_s\right)\right]\vec{\delta}\vec{n}_1 ds \\
&-\rho\iint_{\vec{S}_b}\left(-\vec{U}\cdot\nabla\phi_s + \frac{1}{2}\nabla\phi_s\cdot\nabla\phi_s + gz\right)\vec{n}_2 ds \\
&+\frac{1}{2}\rho g\int_{wl}[\zeta - (\xi_3 + \xi_4 y - \xi_5 x)]^2\frac{\vec{n}_0}{sin\alpha}dl \\
&-\rho\int_{wl}\left[-\vec{U}\cdot\nabla\phi_s + \frac{1}{2}\nabla\phi_s\cdot\nabla\phi_s\right][\zeta - (\xi_3 + \xi_4 y - \xi_5 x)]\frac{\vec{n}_1}{sin\alpha}dl
\end{aligned} \quad (13)$$

where the wave induced motion vector is $\vec{\delta} = \vec{\xi}_T + \vec{\xi}_R \times \vec{x}$, and the vectors $\vec{n}_0$, $\vec{n}_1$ and $\vec{n}_2$ mean the zero, first and second-order components of the normal vector on the hull surface. α represents the angle of the hull flare at free surface.

2.2 Low Frequency Manoeuvring Problem

For the manoeuvring problem, a 3-DOF modular-type model is considered as follows:

$$\begin{aligned}
&(m + m_x)\dot{u} - \left(m + m_y\right)vr - mx_g r^2 = X_H + X_P + X_R + X_W \\
&\left(m + m_y\right)\dot{v} + (m + m_x)ur + mx_g\dot{r} = Y_H + Y_P + Y_W \\
&\left(I_{ZZ} + mx_g^2 + J_{ZZ}\right)\dot{u} + mx_g(\dot{v} + ur) = N_H + N_P + N_W
\end{aligned} \quad (14)$$

where m is the ship mass and I_{ZZ} is the moment of inertia. m_x, m_y and J_{ZZ} are the corresponding added masses and added moment of inertia in surge, sway and yaw, respectively. The subscripts H, P, R of X, Y, N represent the low frequency hydrodynamic forces on the hull, propeller and rudder, respectively; W denotes the mean second order wave drift forces. In the present study, the bare hull related hydrodynamic derivatives in Eq. (14) are determined using a RANS-based solver from STAR CCM+. The other manoeuvring hydrodynamic derivatives for the rudder and the propeller can be found in [1] and [23].

2.3 Numerical Implementation

In this study, the seakeeping problem is solved with a B-spline based time domain higher order Rankine panel method developed by Mei et al [22], while the manoeuvring motion

equations (14) are calculated with a fourth order Runge-Kutta scheme. For the coupling problem of seakeeping and manoeuvring motions, a parallel time marching scheme (the two-time scale) is used, which is following the work of [20]. This means that the global variables, such as ship position and velocity, are firstly calculated in the $O-XYZ$ coordinate system by Eq. (14); then the global variables will be used as input to solve the seakeeping problem under the specified wave condition in the $o-xyz$ coordinate system. Meanwhile, the mean drift forces and moments obtained from seakeeping problem are substituted back to perform the manoeuvring simulation at next time step. The details of the numerical techniques can be found in [20][25].

3 NUMERICAL RESULTS AND DISCUSSIONS

3.1 Test Cases

In order to verify the present method, the S175 container ship is chosen as a case study in present work. The ship main particulars are listed in Table 1.

The wave induced motion of a laterally drifting ship is firstly computed and compared with the numerical and experimental data from [27]. Table 2 shows the computation case in present study. Figure 2 shows the discretized panels on the boundaries in the potential method (full model), where the truncated free surface computational domain is 1.5Lpp upstream, 1.5Lpp downstream and 0.8Lpp half width. The total panels in the numerical domain are 6700, where 1200 are located on the ship's hull and 5500 on the free surface.

Subsequently, the captive model tests (1:50 model scale), see Table 3, including the steady drift test, circular motion test (CMT) and CMT with drift angle test, are carried out by RANSE-based CFD solver STAR-CCM+ to determine hull-related viscous hydrodynamic derivatives. As for the detailed information of the simulation approach and set up in STAR-CCM+ in the present work the reader see the similar work in [26]. Figure 3 shows the rectangular computational domain, where the dimension of computational domain ranges -3Lpp<x<2Lpp, -1.5Lpp<y<1.5Lpp, -1.0Lpp<z<0. It should be noted that the symmetry plane boundary condition is imposed on the top of the domain based on double body model in present study.

Then the turning performance of the S-175 containership in regular waves is studied and the numerical results are compared with the experimental data obtained from [2].

Table 1. MAIN PARTICULARS OF THE S175 CONTAINER SHIP

	Specifications	Full scale	Model
Ship	Length Lpp (m)	175.0	3.500
	Beam $B(m)$	25.4	0.508
	Draft $T(m)$	9.5	0.190
	Froude number Fr	0.15	0.15
	Radius of gyration k_{xx}/B	0.328	0.328
	Radius of gyration k_{xx}/Lpp,k_{yy}/Lpp	0.24	0.24
	Longitudinal centre of gravity (m)	-2.545	-0.051
	Vertical centre of gravity (m)	9.52	0.1904
Propeller	Propeller diameter(m)	6.507	0.1301
	Pitch ratio	0.7348	0.7348
Rudder	Area (m^2)	32.46	0.0130
	Span length (m)	7.7	0.154
	Chord length (m)	4.215	0.0843

Table 2. COMPUTATION CASE FOR THE LATERALLY DRIFTING S175 CONTAINER SHIP

Item	Computation case
Wave angle (χ)	180°
Heading angle (ψ_0)	0°
Drift angle (β)	0°, 5°, 10°
Forward speed (Fr**)**	0.15
Wave amplitude (ζ_A)	1.75m
Wave frequency (λ/Lpp)	0.25 ~ 2.1

Table 3. COMPUTATION CASE FOR VIRTUAL CAPTIVE MODEL TESTS OF S175 CONTAINER SHIP

Item	$\boldsymbol{\beta}$ $(\boldsymbol{v'=-sin\beta})$	$\boldsymbol{r'}$	Hydrodynamic coefficients
Steady drift tests	0°, 4°, 6°, 8° ,12°, 16°	0	X'_{vv}, Y'_{vvv}, Y'_v, N'_{vvv}, N'_v
CMTs	0°	0, 0.2, 0.4, 0.6	X'_{rr}, Y'_{rrr}, Y'_r, N'_{rrr}, N'_r
Combined tests	0°, 4°, 6°, 8° ,12°, 16°	0, 0.2, 0.4, 0.6	X'_{vr}, Y'_{vvr}, Y'_{vrr}, N'_{vvr}, N'_{vrr}

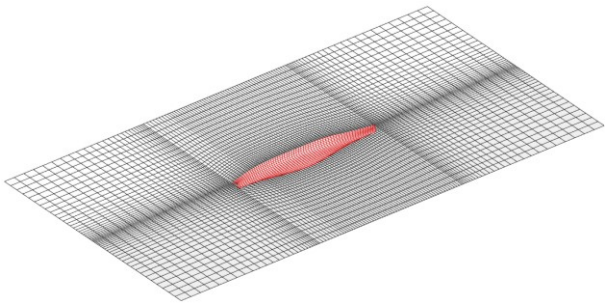

FIGURE 2: DISCRETIZED PANELS ON HULL AND FREE SURFACES

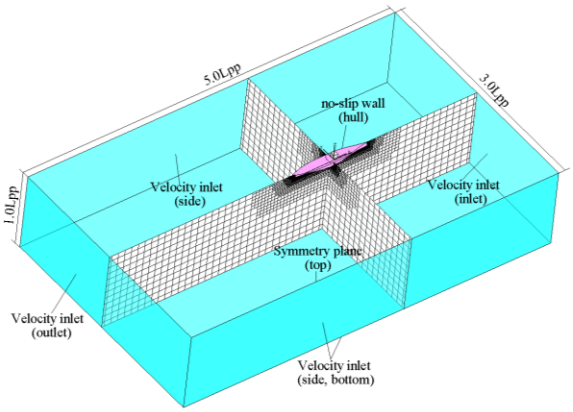

FIGURE 3: COMPUTATIONAL DOMAIN AND BOUNDARY CONDITIONS USING DOUBLE-BODY METHOD

3.2 Wave Induced Motion of a Laterally Drifting Ship

In order to validate the present code and compare with the available experimental results in [27], the wave induced motion of the laterally drifting S175 container ship will be calculated for the computation case in Table 2.

Figure 4 shows the numerical results of wave induced motion responses in head waves for different drift angles in comparison with the 2D strip method and experimental data by Yasukawa et al. [27]. Note that the surge motion in [27] is not considered due to the use of the strip theory.

As can be seen from Figure 4, generally the present numerical results show better agreement with experimental data than that by 2D strip method except for the sway motion. One reason, as explained in [27], might be the insufficient wave exciting roll moment acting on the laterally drifting ship in head waves; secondly the amplitude of sway motion is actually a smaller quantity compared with other DOF's in head waves, therefore accurate prediction seems to be even more difficult. Another crucial factor may be the present potential method, which does not sufficiently consider lift effects when meeting larger drift angles, such as vortex around transom stern and bulbous bow. The problem may be to properly dealt with by implementing the Kutta condition and will be considered in further studies.

Another important observation is that, as seen in Figure 4 (c) and (d), the heave and pitch motions in head waves do not significantly change when the drift angle is considered, this is observed for both numerical and experimental results. The reason behind this is that there is no change in the added mass, the damping coefficients, and the exciting forces due to lateral drift.

Figure 5 shows the wave contours around S175 container ship for the drift angles $\beta = 0°,\ 5°,\ 10°$. From Figure 5 one can clearly observe asymmetry and this increases with the increase of drift angle. The reason is the existing of the drift angle which changes the distribution of flow field around the ship, as a result, the disturbance wave is no more symmetrical in comparison to the case with no drift angle in head waves.

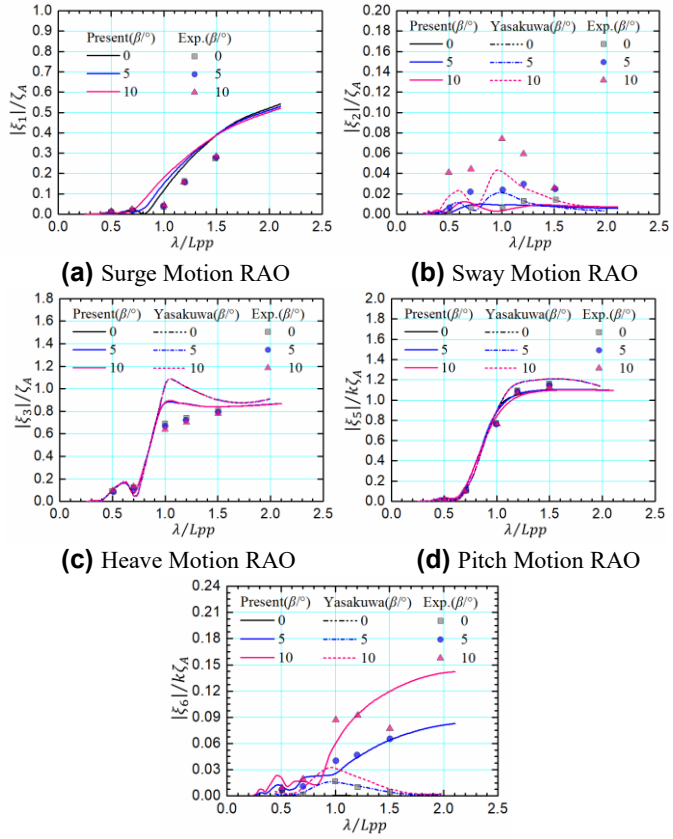

(a) Surge Motion RAO **(b)** Sway Motion RAO

(c) Heave Motion RAO **(d)** Pitch Motion RAO

(e) YAW MOTION RAO

FIGURE 4: COMPARISON WAVE INDUCED MOTION RESPONSES IN HEAD WAVES FOR DIFFERENT DRIFT ANGLES

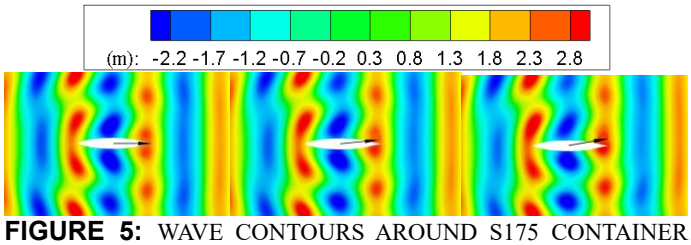

FIGURE 5: WAVE CONTOURS AROUND S175 CONTAINER SHIP. $\beta = 0°$ (LEFT), $\beta = 5°$ (MIDDLE) AND $\beta = 10°$ (RIGHT). $Fr = 0.15$

3.3 Manoeuvring Hydrodynamic Derivatives

Figure 6 presents the normalized results of hydrodynamic forces and moments on the bare hull by the virtual captive model tests (see Table 3), where the forces and moments are normalized by $0.5\rho U^2 LT$ and $0.5\rho U^2 L^2 T$, respectively. By using the least-squares fitting method, the velocity dependent hydrodynamic derivatives (i.e. X'_{vv}, Y'_{vvv}, Y'_v, N'_{vvv} and N'_v) can be determined from steady drift tests; similarly, the angular velocity dependent hydrodynamic derivatives (i.e. X'_{rr}, Y'_{rrr}, Y'_r, N'_{rrr} and N'_r) can be determined by CMTs; the coupled derivatives (i.e. X'_{vr}, Y'_{vvr}, Y'_{vrr}, N'_{vvr} and N'_{vrr}), it can be determined from a combination of the CMT and steady drift tests. As for other related hydrodynamic derivatives and coefficients used in

the present study, the values are obtained from the experiment data available in [23].

Table 4 shows the normalized results of hull-related hydrodynamic derivatives determined from the present CFD computations and are compared with the results obtained in [1] and [23]. Note that the hydrodynamic derivatives used in calculations in [1] are inferred from the experimental results in [23] , because the drafts in [1] and [23] correspond to 9.5m and 8.5m for full scale, respectively. As can be seen from Table 4, though some deviations can the found, especially for X'_{rr}, other angular velocity dependent hydrodynamic derivatives (i.e. Y'_{rrr}, Y'_r, N'_{rrr} and N'_r) still show good agreement with [1]. As for the rest of the calculated manoeuvring derivatives, they are need to be further validated but no experimental results are available for these cases. Furthermore, as explained in He et al. [24], the CFD approach is sensitive to many factors, such as mesh, motion parameters and so on, the reliability of CFD method still required to be further investigated.

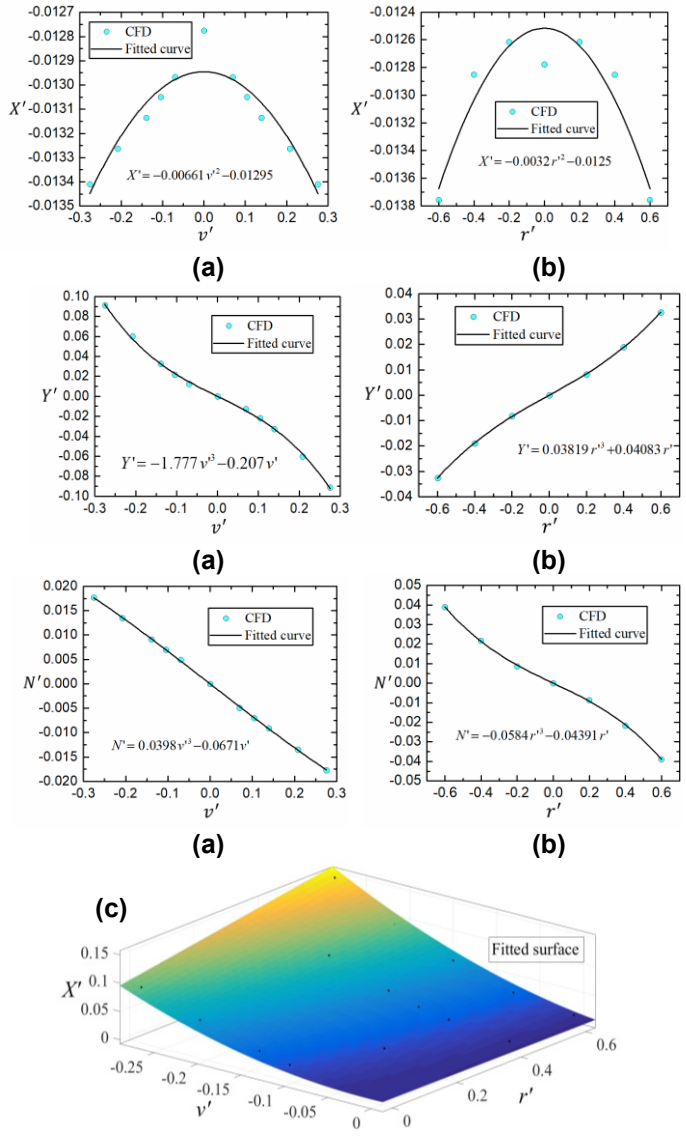

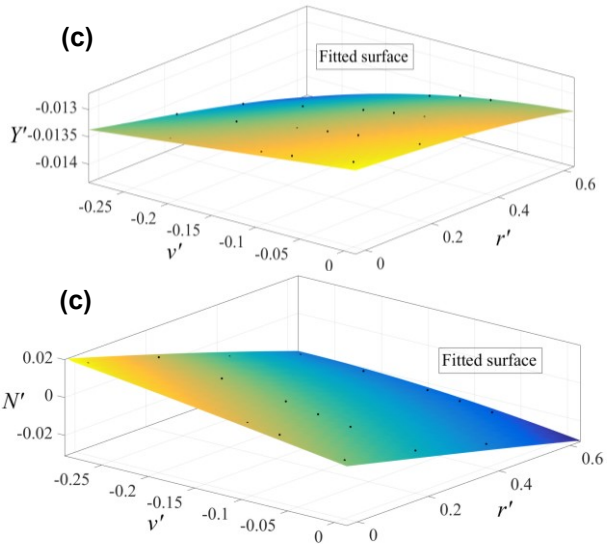

FIGURE 6: HYDRODYNAMIC FORCES ON THE BARE HULL. (a) STATIC DRIFT TESTS; (b) CMTS; (c) CMTS WITH DRIFT ANGLE TESTS.

TABLE 4. COMPARISON OF MANOEUVRING DERIVATIVES

Derivatives	Present CFD	[1]	Exp. [23]
X'_{vv}	-0.0066	-	-0.00386
Y'_v	-0.207	-	-0.0116
Y'_{vvv}	-1.777	-	-0.109
N'_v	-0.0671	-	-0.00385
N'_{vvv}	0.0398	-	0.001492
X'_{rr}	-0.0032	0.0037	0.0002
Y'_r	0.04083	0.0446	0.00242
Y'_{rrr}	0.03819	0.0326	0.00177
N'_r	-0.04391	-0.0409	-0.00222
N'_{rrr}	-0.0584	-0.0422	-0.00229
X'_{vr}	-0.03256	-	-0.00311
Y'_{vvr}	-0.0108	-	0.0214
Y'_{vrr}	-0.00865	-	-0.0405
N'_{vvr}	-0.1383	-	-0.0424
N'_{vrr}	0.01595	-	0.00156

3.4 Turning Performance in Regular Waves

Figure 7 and Figure 8 show the comparisons of port turning trajectories in regular beam and head waves at $\lambda/L\,pp = 0.7, 1.0$, wave amplitude $\zeta_A = 1.75m$. In these figures the experimental data from [2] and the numerical results in [18] are also displayed. Note that the speed of ship is $Fr = 0.15$, the propeller revolution is 1.42rps [18], and the rudder speed rate is set to 3.5°/s.

From both figures it can be seen that in general the present numerical result can roughly predict the turning trends in regular waves, which demonstrates the present hybrid method has a good applicability as the method in [18]. But as can be seen from the figures, some obvious deviations can be found, especially for the cases in the initial beam wave scenario. The reason may be

the errors due to the numerical technique in present study, but this needs to be further investigated.

By comparing the results shown in Figure 7(a) with Figure 7(b), Figure 8 (a) with Figure 8 (b) separately, we can find that the shorter the wavelength, the longer the drift distance is. This phenomenon might be accounted for the fact that larger lateral drift forces and yaw moments will be induced by short wavelength than in relatively long wavelength. In addition, as shown in the figures, when a ship is turning in regular waves, the trajectory does not necessarily drift towards the wave propagating direction, but with a drifting angle with respect to incident wave direction, the same conclusion can also be found in [2], [3] and [18]. The main characteristics of turning circles in waves can be characterized by the drifting distance and the drifting direction, which are detailed depicted in [3]. In this sense, the accuracy of predicting the turning circle in waves depends greatly on the accuracy of the second order drift force and yaw moment.

Additionally, initial incident wave angles also have considerable effect on the turning trajectories. As can be seen from comparisons for the corresponding wavelengths in the figures, i.e. Figure 7(a) and Figure 8 (a) at $\lambda/Lpp = 0.7$, Figure 7(b) and Figure 8 (b) at $\lambda/Lpp = 1.0$, when the initial wave angle is 180° in Figure 8, the negative effect of added resistance will lead to a speed loss when keeping a constant initial output power, subsequently the thrust force will decrease so that the waves force the ship making a faster turn than that in initial wave angle is 90° in Figure 7.

Figure 9 shows the normalized time histories of wave induced heave and pitch motions in contrast to the experimental results in [2] during port turning in beam waves ($\chi = 90°$) at $\lambda/Lpp = 0.7$. Figure 10 only represents the present numerical time histories of wave induced heave and pitch motions during port turning in head waves ($\chi = 180°$) at $\lambda/Lpp = 0.7$ due to the lack of available experimental data for comparison. As can be seen in Figure 9, present numerical results (blue line) can roughly capture the changes of wave induced motion amplitude, but the deviations of phase angles for crests and troughs can be found in comparison with experimental results (red line), the reason is that the high frequency seakeeping problem is dependent on encounter frequency, which reflects the effect from manoevring problem. But in fact, the differences exist (including the magnitude and phase angle) between the numerical and experimental results due to the numerical errors and technics used by present potential method. Despite the numerical errors, the present prediction method can still be used as a qualitative analysis at the initial research stage.

Figure 11 gives the present numerical results of normalised forward and lateral speed during turning motion. As can be seen, the components of speed also show the oscillation characteristics when performing a turning circle, which reflects the influence of waves. In addition, the lateral speed component seems to be of a smaller magnitude compared to the forward speed component. This conclusion also explains why some researcher neglect the influence of lateral velocity and just suppose the ship velocity U can be approximated by the surge velocity u, i.e. [21].

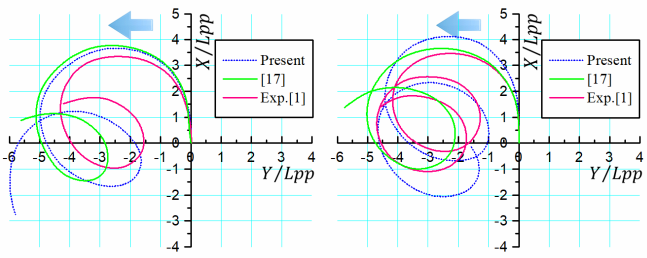

(a) $\lambda/Lpp = 0.7$ **(b)** $\lambda/Lpp = 1.0$

FIGURE 7: PORT TURNING TRAJECTORIES IN BEAM WAVES

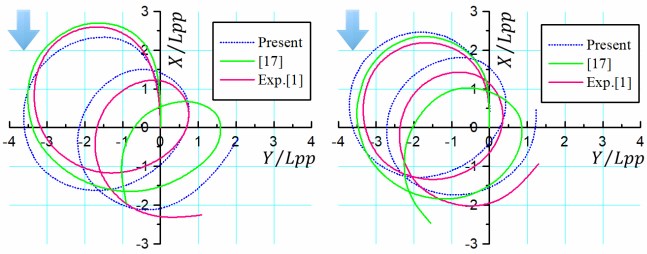

(a) $\lambda/Lpp = 0.7$ **(b)** $\lambda/Lpp = 1.0$

FIGURE 8: PORT TURNING TRAJECTORIES IN HEAD WAVES

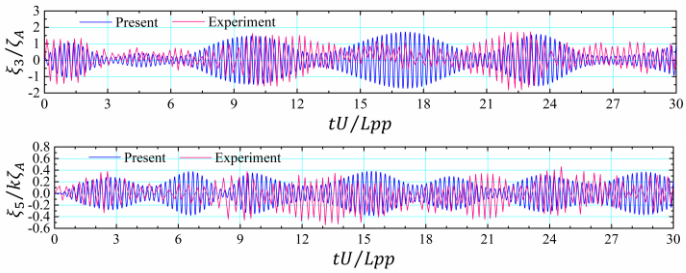

FIGURE 9: WAVE INDUCED HEAVE AND PITCH MOTIONS DURING PORT TURNING TRAJECTORIES IN HEAD WAVES ($\delta = 35°$, $\chi = 90°$, $\lambda/L = 0.7$)

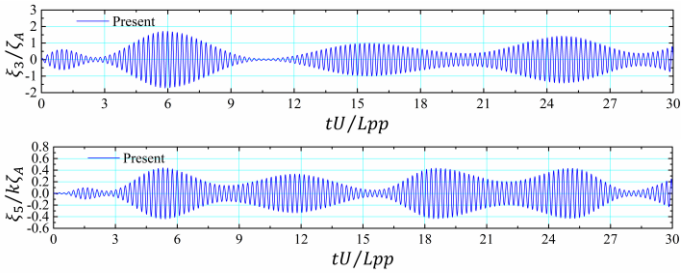

FIGURE 10: WAVE INDUCED HEAVE AND PITCH MOTIONS DURING PORT TURNING TRAJECTORIES IN HEAD WAVES ($\delta = 35°$, $\chi = 180°$, $\lambda/Lpp = 0.7$)

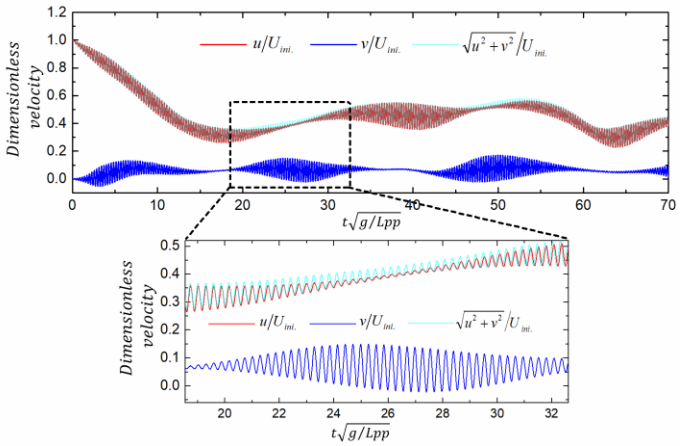

FIGURE 11: FORWARD AND LATERAL SPEED DURING PORT TURNING TRAJECTORIES IN HEAD WAVES ($\delta = 35°$, $\chi = 180°$, $\lambda/Lpp = 1.0$)

4 CONCLUSION

In the present work, a hybrid method, combing potential theory and CFD method, is applied for the prediction of ship's manoeuvring behaviour in regular waves. The two-time scale method is then applied to integrate the seakeeping model with lateral speed and yaw rate in a 3-DOF MMG model to evaluate the turning circle and wave induced motions during turning. From the results and comparisons with model test resuts, the following conclusions can be obtained:

1) The 3D time domain Rankine panel method containing the effects of forward speed and lateral speed developed in this study can be used as a practical way to evaluate the seakeeping problem of laterally drifting ship, but the accuracy will probably be improved by implementing the Kutta condition when adding vortex related viscous effects.

2) Combining potential theory with CFD techniques can be used efficiently for predicting the manoeuvring behaviour in waves in the case of lacking manoeuvring derivatives and coefficients provided from experimental data.

3) In the presence of waves, the turning trajectory does not necessarily drift towards the wave propagating direction, but with a drifting angle with respect to incident wave direction, what is more, the shorter the wavelength, the longer the drift distance is. From this perspective, the accuracy of second order drift force and yaw moment solved in seakeeping problem has critical effect on prediction of turning circle in waves

ACKNOWLEDGEMENTS

This work was supported by the Lloyd's Register Foundation (LRF) and China Scholarships Council (CSC). LRF and CSC help to protect life and property by supporting engineering-related education, public engagement and the application of research.

REFERENCES

[1] Yasukawa, H., 2006. "Simulations of ship maneuvering in waves (1st report: turning motion)", *Journal of the Japan Society of Naval Architects and Ocean Engineers*, 4, pp. 127-136.

[2] Yasukawa, H., and Nakayama, Y., 2009, "6-DOF motion simulations of a turning ship in regular waves", In *Proceedings of the International Conference on Marine Simulation and Ship Manoeuvrability*, pp: 508-517.

[3] Ueno, M., Nimura, T., and Miyazaki, H., 2003, "Experimental study on manoeuvring motion of a ship in waves", In *International Conference on Marine Simulation and Ship Maneuverability*, MARSIM'03, Kanazawa, pp: 664-670.

[4] Lee, S., Hwang, S., Yun, S. W., Rhee, K. P., and Seong, W. J., 2009, "An experimental study of a ship manoeuvrability in regular waves", *In International Conference on Marine Simulation and Ship Maneuverability*, Panama, pp. 17-23.

[5] Yasukawa, H., Hirata N., Yonemasu, I., Terada, D., and Matsuda, A., 2015. "Maneuvering simulation of a KVLCC2 tanker in irregular waves", *In: Proceedings of International Conference on Marine Simulation and Ship Manoeuvrability*, Newcastle, UK.

[6] Sprenger, F., Maron, A., Maron, A., Delefortrie, G., Van Zwijnsvoorde, T., Cura-Hochbaum, A., Lengwinat, A., and Papanikolaou, A., 2017, "Experimental Studies on Seakeeping and Maneuverability of Ships in Adverse Weather Conditions", *Journal of Ship Research*, 61(3), 131-152.

[7] Mousaviraad, M., Bhushan, S., and Stern, F., 2012, "CFD Prediction of Free-Running SES/ACV Deep and Shallow Water Maneuvering and Course-Keeping in Calm Water and Waves", *International Conference on Marine Simulation & Ship Manoeuvrability*.

[8] Cura Hochbaum, A., and Uharek, S., 2016, "Prediction of Ship Manoeuvrability in Waves Based on RANS Simulations", *31st Symposium on Naval Hydrodynamics*, Monterey, California, pp. 11-16.

[9] Wang, J. H., Zou, L., and Wan, D. C., 2017, "CFD simulations of free running ship under course keeping control", *Ocean Engineering*, 141,pp. 450-464.

[10] Wang, J. H., Zou, L., and Wan, D. C., 2018, "Numerical simulations of zigzag maneuver of free running ship in waves by RANS-Overset grid method", *Ocean Engineering*, 162, pp. 55-79.

[11] Bailey, P. A., Price, W. G., and Temarel, P., 1997, "A unified mathematical model describing the maneuvering of a ship travelling in a seaway", *Transactions of The Royal Institution of Naval Architects*, 140, pp. 131-149.

[12] Fossen, T.I., 2005, "A nonlinear unified state-space model for ship maneuvering and control in a seaway", *International Journal of Bifurcation and Chaos*, 15(09), pp. 2717-2746.

[13] Sutulo, S. and Soares, C. G., 2008, "A generalized strip theory for curvilinear motion in waves", *In ASME 2008 27th International Conference on Offshore Mechanics*

and Arctic Engineerin, 6, pp. 359-368.
[14] Schoop-Zipfel, J., and Abdel-Maksoud M. A., 2011, "A Numerical Model to Determine Ship Maneuvering Motion in Regular Waves", *In Proceedings of the International Conference on Computational Methods in Marine Engineering (MARINE)*.
[15] Subramanian, R., and Beck, R. F., 2015, "A time-domain strip theory approach to maneuvering in a seaway", *Ocean Engineering*, 104, pp. 107-118.
[16] Skejic, R., and Faltinsen, O. M., 2008, "A unified seakeeping and maneuvering analysis of ships in regular waves", *Journal of marine science and technology*, 13(4), pp. 371-394.
[17] Yasukawa, H., Hirata, N., Matsumoto A., Kuroiwa R., and Mizokami S., 2017, "Evaluations of wave-induced steady forces and turning motion of a full hull ship in waves", *Journal of Marine Science and Technology*, pp. 1-15.
[18] Seo, M. G., and Kim, Y., 2011, "Numerical analysis on ship maneuvering coupled with ship motion in waves", *Ocean engineering*, 38, pp. 1934-1945.
[19] Seo, M. G., Nam, B. W., and Kim, Y. G., 2018, "Numerical Evaluation of Ship Maneuvering Performance in Waves", *In ASME 2018 37th International Conference on Ocean, Offshore and Arctic Engineering*, pp: V07AT06A002-V07AT06A002.
[20] Zhang, W., Zou, Z. J., and Deng, D. H., 2017, "A study on prediction of ship maneuvering in regular waves", *Ocean Engineering*, 137, pp. 367-381.
[21] Chillcce, G., and el Moctar, O., 2018, "A numerical method for manoeuvring simulation in regular waves", *Ocean Engineering*, 170, pp. 434-444.
[22] Mei, T. L., Zhang, T., Zou, Z. J., Lataire, E.,and Vantorre, M. "Comparative study on ship motions in waves based on two time domain panel methods", *To be submitted*.
[23] Son, K., and Nomoto, K., 1981, "On the coupled motion of steering and rolling of a high speed container ship", *Journal of the Society of Naval Architects of Japan*, 1981(150), pp. 232-244.
[24] He, S., Kellett, P., Yuan, Z., Incecik, A., Turan, O., and Boulougouris, E., 2016, "Manoeuvring prediction based on CFD generated derivatives", *Journal of Hydrodynamics*, 28(2), pp. 284-292.
[25] Zhang, W., 2016, "A research on numerical prediction of ship maneuverability in regular waves", Ph.D. Thesis, Shanghai Jiaotong Unversity. (in Chinese).
[26] Liu Y., 2018, "CFD-based Studies on Virtual Captive Model Tests of Ship Manoeuvring", Ph.D. Thesis, Shanghai Jiaotong Unversity. (in Chinese).
[27] Yasukawa, H., Amri Adnan, F., and Nishi, K., 2010, "Wave-Induced Motions on a Laterally Drifting Ship", *Ship Technology Research*, 57(2), pp. 84-98.